Journal of Catalysis **186,** 362–372 (1999)
Article ID jcat.1999.2567, available online at http://www.idealibrary.com on IDEAL®

# A Transient Kinetic Study of the Mechanism of the $NO + H_2$ Reaction over $Pt/SiO_2$ Catalysts

## 2. Characteristic Features of SSITKA Profiles

A. A. Shestov,[1] R. Burch, and J. A. Sullivan

*Catalysis Research Centre, Chemistry Department, University of Reading, Whiteknights, Reading, RG6 6AD, United Kingdom*

Received February 4, 1999; revised May 11, 1999; accepted May 11, 1999

**SSITKA profiles obtained for the $NO + H_2$ reaction on a 5% $Pt/SiO_2$ catalyst at low temperatures are analysed in an attempt to gain insight into the reaction mechanism at the molecular level, specifically for the formation of $N_2$, $N_2O$, and $NH_3$. Three different analyses are introduced which give information about the nature of the reaction network and the final intermediates on the Pt surface under reaction conditions. These are (a) the initial distribution of isotopic molecules of product (IDIMP), (b) the temporal redistribution of isotopic molecules of product (TRIMP), and (c) the semilogarithmic plot of ($\tilde{\alpha}$) versus time. The first two analyses (IDIMP and TRIMP) are discussed in terms of "types of production" of two atom labelled product molecules. We also introduce the integral characteristics of a reaction mechanism, i.e., the coefficient of percolation ($C_{PE}$) and the coefficient of production ($C_{PR}$). The conclusions, along with the experimental data, are used to develop a reaction mechanism for the formation of $N_2$, $N_2O$, and $NH_3$ from Pt catalysts in the $NO + H_2$ reaction.** 

*Key Words:* **NO reduction; SSITKA; modelling; reaction mechanism; Pt catalysts.**

### INTRODUCTION

Steady state isotope transient kinetic analysis (SSITKA) has previously been used to clarify the mechanisms of several reaction types, e.g., Fischer–Tropsch synthesis (1), CO hydrogenation (2), $NH_3$ oxidation (3), oxidative coupling of $CH_4$ (OCM) (3, 4), methanol synthesis (5), CO oxidation and CO/NO reaction (6, 7), $NO/NH_3$ reactions (8, 9), $NO/CH_4$ (10) reactions, and $NO/C_3H_6/O_2$ reactions (11, 12). As a general rule the reactions which provide the clearest information are those in which the surface contains large reservoirs of adsorbed intermediates which are slowly transformed to products.

In the present work, SSITKA is used to study the $NO + H_2$ reaction over one such supported Pt catalyst (5% $Pt/SiO_2$) in an attempt investigate the nature of the surface intermediates in the formation of $N_2$ and $N_2O$. The previous paper (13) considered "classical" quantitative analysis of SSITKA profiles and resulted in the generation of values for such parameters as surface coverages and reactivity of intermediates.

Since the development of the SSITKA technique, by Happel (14), Bennett (15), and Biloen (16), there have been many articles devoted to the numerical analysis of such profiles with the aim of generating information about reaction mechanisms. These numerical analyses have generally taken the form of modelling the transient data generated from either continuously stirred tank (17, 18) or plug flow (19) reactors. Comprehensive reviews of the technique have been published (20, 21). However, it is generally the case that most workers have analysed isotope transfer only, i.e., the fraction of isotopes within the components with time. Distribution of isotopic molecules has been disregarded or only partially considered without detailed qualitative analysis of experimental data (4).

In this paper we introduce and develop several methods of analysing the data obtained from isotopic transients in order to try to suggest an unambiguous reaction mechanism. Some features of these methods originally come from classical isotopic exchange analysis in closed systems without the occurrence of chemical changes in the system (22–29).

Specifically our approach will be for situations where a reactant molecule ($RA_n$) containing labelled atoms (where there are two possible isotopes for the A element) is converted, via intermediates ($IA_x$), into a product molecule that contains two such labelled atoms ($PA_2$) for a steady state reaction in a plug flow reactor, e.g., $^*NO + H_2 \rightarrow {}^*N_2/{}^*N_2O$, $^*NH_3 + O_2 \rightarrow {}^*N_2/{}^*N_2O$, $^*CH_4 + O_2 \rightarrow {}^*C_2H_4/{}^*C_2H_6$, $^*O_2 + Ph\text{–}CH_3 \rightarrow Ph\text{–}C^*O^*OH$, where an asterisk represents a labelled atom. A full mathematical description of the methodology used in the interpretation and modelling of these results is presented elsewhere (30). Only the essential details are given here.

Three different analyses (and transformations) of the experimental profiles for the $NO + H_2$ reaction will be

[1] On leave from Boreskov Institute of Catalysis, Russian Academy of Sciences, Pr. Akademika Lavrentieva, 5, Novosibirsk, 630090, Russia.



0021-9517/99 $30.00

discussed in relation to the information they yield about the mechanism of the $N_2$ and $N_2O$ forming reactions. These analyses are (a) the initial distribution of isotopic molecules of product (IDIMP), (b) the temporal redistribution of the isotopic molecules of product (TRIMP) (i.e., the function $y_{(i)}$, the deviation from statistical isotopic distribution within the product molecules), and (c) a semilogarithmic plot of the $\bar{\alpha}$ function (where $\bar{\alpha}$ represents the $(1-\alpha)$ profile in the case of a $^{14}NO \rightarrow {}^{15}NO$ switch and the $\alpha$ profile in the case of the reverse $^{15}NO \rightarrow {}^{14}NO$ switch) versus time. As detailed previously, $\alpha$ is the fraction of heavy atoms in the gas phase (13), e.g., $\alpha$ for $N_2$ can be calculated using the equation

$$\alpha(N_2) = \frac{[^{15}N_2] + 0.5[^{15}N^{14}N]}{[^{15}N_2] + [^{14}N^{15}N] + [^{14}N_2]}. \qquad [1]$$

Plot (a) is a "snapshot" of the initial redistribution immediately following a $^{14}NO + H_2 \rightarrow {}^{15}NO + H_2$ switch while plots (b) and (c) are presented as a function of time. Note that IDIMP has been used previously for studying reactions such as benzene hydrogenation in open systems (31, 32).

Profiles (a) and (b) are discussed in terms of the concept of "types of production" of two atom labelled molecules ($PA_2$) as discussed later. The first set of plots are also used to introduce the concept of the integral characteristics of any network mechanism of the form $RA_n \rightarrow \cdots IA_x \cdots \rightarrow PA_2$, i.e., where a labelled reactant ($RA_n$) progresses through one or more surface intermediates ($IA_x$) to yield a 2-atom labelled molecule ($PA_2$).

## EXPERIMENTAL

The SSITKA switches are performed at 60°C under similar conditions to those used in the previous paper (13). The conditions are altered somewhat to enhance the resolution and to ensure that the pressure changes on switching are minimised. The gas composition used was 3% NO, 3% $H_2$ in a total flow of 62 $cm^3\ min^{-1}$. The catalyst was the same as used previously, i.e., 5% $Pt/SiO_2$. Data analysis and the generation of the various functions was performed on a bench-top PC using a commercial spreadsheet program.

## TYPES OF PRODUCTION OF TWO-ATOM LABELLED MOLECULES

In order to discuss the first and second transformations of the data, we have to first introduce the concept of "types of production." This involves differentiating steady state reaction mechanisms on the basis of the final reaction step leading to the generation of the product molecule ($PA_2$) from the reactant ($RA_n$) and any final intermediates on the surface ($IA_x$ or $I'A_x$) which go on to form $PA_2$.

Detailed analysis (30) of the modes in which a molecule of product ($PA_2$) containing two "labellable" A atoms can be formed from a labelled reactant molecule ($RA_n$) and intermediates $IA_x$ has shown that there are basically five "pure" types of production of such molecules. These are shown in Table 1 and briefly discussed below. In the following discussion, A represents a labelled atom (with two possible isotopes), $RA_n$ represents a reactant containing "$n$" such atoms, $PA_2$ represents a product containing two such A atoms, and $IA_x$ represents an intermediate containing "$x$" A atoms. R, P, and I are parts of the molecule that do not contain any A atoms (or contain A atoms that remain unreactive). We will consider a singly labelled reactant (RA) and either singly or doubly labelled intermediates (IA and $IA_2$) to simplify the types of production which we will discuss.

The first type of production (labelled 0) is one in which the surface plays no discernible role and the production of $PA_2$ involves no surface A atoms, i.e.,

$$\text{type 0} \quad 2RA \rightarrow PA_2. \qquad [2]$$

The second type (labelled 1) involves, for example, an impact mechanism in which a molecule of RA interacts with

**TABLE 1**

**Designation of the Five Possible Types of Production of a Product Molecule $PA_2$ from a Reactant Molecule RA and Reaction Intermediates (IA and I′A), Showing the Final Reaction Steps**

| Type of production | Mechanism | Temporal redistribution $y_i = x_i - x_i^{eq}$ | Initial distribution $\{x_0^0, x_1^0, x_2^0\}$ | Production coefficient $C_{PR}$ | Percolation coefficient $C_{PE}$ |
|---|---|---|---|---|---|
| 0 | $2RA \rightarrow PA_2$ | $y_1 = y_2 = 0$ | {0, 0, 1} | 0 | 2 |
| 1 | $RA + IA \rightarrow PA_2$ | $y_1 > 0, y_2 < 0$ | {0, 1, 0} | 1 | 1 |
| 2a | $2IA \rightarrow PA_2$ | $y_1 = y_2 = 0$ | {1, 0, 0} | 2 | 0 |
| 2b | $IA + I'A \rightarrow PA_2$ | $y_1 > 0, y_2 < 0$ | {1, 0, 0} | 2 | 0 |
| 2c | $IA_2 \rightarrow PA_2$ | $y_1 < 0, y_2 > 0$ | {1, 0, 0} | 2 | 0 |

*Note.* Also shown are the predicted temporal redistributions of the isotopically labelled molecules ($(PA^*A^*$ and $PAA^*)$) the expected initial isotopic distribution following the same switch, and the expected production ($C_{PR}$) and percolation ($C_{PE}$) coefficients following a step change $RA \rightarrow RA^*$ (see text for details).

a surface intermediate which gives one A atom to produce a $PA_2$ molecule. This involves one surface A atom in the elementary act of production of $PA_2$, i.e.,

$$\text{type 1} \quad RA + IA \rightarrow PA_2. \qquad [3]$$

The third, fourth, and fifth methods of formation of $PA_2$ all involve two surface A atoms in the act of production. These are thus labelled "2" and are differentiated on the basis of the types of 2-atom interactions. Production type 2a (a for alone) represents the formation of a $PA_2$ molecule from two equivalent species on the surface both of which give one A atom to the final product, i.e.,

$$\text{type 2a} \quad 2IA \rightarrow PA_2. \qquad [4]$$

Production type 2b (b for binary) represents the formation of $PA_2$ from the interaction of two different species on the surface, both of which give one A atom to the final product, i.e.,

$$\text{type 2b} \quad IA + I'A \rightarrow PA_2. \qquad [5]$$

The final type of production of $PA_2$ is type 2c (c for coupled) and this involves the presence of a "coupled" intermediate on the surface which contains, as a minimum, two A atoms. Both atoms that go on to form $PA_2$ originate from the same species, i.e.,

$$\text{type 2c} \quad IA_2 \rightarrow PA_2. \qquad [6]$$

These different types of production lead to different responses in the above-mentioned first and second features of the obtained profiles, i.e., initial distribution of isotopic molecules of product (IDIMP) and temporal redistribution of isotopic molecules of product (TRIMP). The expected outcomes of the above-mentioned transformations from any "pure" type of production (0, 1, 2a, 2b, or 2c) are also detailed in Table 1 and are further discussed below. It must be remembered that these formalisms do not necessarily represent actual reactions but rather just "modes" of reaction and that the action of any type can lead to different profiles which depend on factors such as surface concentrations, rates, and reversibility of steps. However, the temporal redistribution and initial distribution plots developed for every type of production must have the same qualitative individual features as are discussed below.

It must also be noted here that for a considered type of production the atomicity of the surface intermediates ($IA_x$) is unimportant and the individual features of IDIMP and the qualitative features of TRIMP will remain the same; e.g., $IA_2 + I'A_2 \rightarrow PA_2 + IA + I'A$ also represents a type 2b production and $IA_3 \rightarrow PA_2 + IA$ represents type 2c production and will give the corresponding IDIMP and qualitative TRIMP features. Additionally, we must allow for isotopic exchange of the product molecules (through adsorption/desorption processes) with either the final intermediates or with different sites on the surface. In these cases the situation becomes more complex, and these will not be considered further here (see (30)). For many experimental cases regarding molecules such as $N_2$ and $N_2O$ these exchange reactions are not important.

In terms of the types of productions we can also say that the overall rate of production of the two-atom molecule equals the sum of the rates of the five types of production (in a normalised form at a value of 1),

$$\chi_0 + \chi_1 + \chi_{2a} + \chi_{2b} + \chi_{2c} = 1, \qquad [7]$$

where $\chi_k$ represents the contribution of type $k$ ($k = 0$, 1, 2a, 2b, 2c), with a rate $R_k$, in the overall production (with a rate $R_\Sigma$); therefore, $\chi_k = R_k/R_\Sigma$. The strict method of calculating $\chi_k$ on the basis of isotopic kinetic equations will be presented later (30). A second, less accurate but simpler method, based on IDIMP, will be discussed below.

## CHARACTERISTIC FEATURES OF SSITKA PROFILES

This section will be divided into the three subsections. Each section will be introduced separately. The results will be discussed, both in general and more specifically for our experimental system, in terms of the information yielded about the nature of the surface intermediates and the reaction network.

### *a. Initial Distribution of Isotopic Molecules of Product (IDIMP) and Integral Characteristics of the Network Mechanism*

Here we will re-introduce and revise a method of analysis previously proposed by Kemball (22) for the analysis of isotopic heteroexchange $C_nH_m$–$D_2$ exchange and also introduce the integral characteristics of a network mechanism.

If we consider the overall production of an isotopic product molecule containing two "labellable" atoms following the $RA + () \rightarrow {}^*RA + ()$ switch within the SSITKA analysis, there are normalised connections for the initial distribution of the isotopic molecules of product, e.g.,

$$x_0^0 + x_1^0 + x_2^0 = 1 \qquad [8]$$

(where $x_i^0$ represents the initial fraction of isotopic molecules which contain $i$ heavy atoms, e.g., $^{14}N_{2-i}{}^{15}N_i$). The overall production of $N_2$ remains constant. Therefore, the sum of the fractions of all isotopic molecules must, at all times, equal a normalised value of 1.

The initial isotopic product distribution following the $RA + () \rightarrow R^*A + ()$ switch (in our case the $^{14}NO + H_2 \rightarrow {}^{15}NO + H_2$) is different for some of the types of production of $PA_2$. Type 0 results in the initial distribution being fully doubly labelled, while type 1 production would lead to fully singly labelled, and all the type 2 productions (2a,

2b, and 2c) would lead to unlabelled product molecules in the initial isotopic distribution (see Table 1).

There are connections between the initial isotopic distribution and the contributions of the different types of production. If the probability (or contribution) of type of production $k$ is $\chi_k$ and the initial isotopic distribution is represented as $\{x_0^0, x_1^0, x_2^0\}$, then it can be shown that

$$x_0^0 = \chi_{2a} + \chi_{2b} + \chi_{2c} \quad [9]$$

$$x_1^0 = \chi_1 \quad [10]$$

$$x_2^0 = \chi_0, \quad [11]$$

that is to say that the initial distribution gives direct information about the contributions of various types of production to the overall production of $PA_2$.

Obviously these are theoretical calculations, and it can be shown (30) that the imposition of an experimental switch rather than an ideal switch from $^{14}NO$ to $^{15}NO$ does change this distribution somewhat. In the specific case of the NO + $H_2$ reaction over Pt/$SiO_2$ this makes any IDIMP analysis of the $N_2O$ distribution more prone to errors as this is very rapid relative to the $N_2$ redistribution and thus more prone to effects of the imposed "experimental" switch. Generally then, with respect to the gaseous holdup of the system, the "shorter" the holdup the more accurate the IDIMP.

IDIMP plots are constructed, for our experimental system, by taking the normalised values for all the isotopic molecules of $N_2O$ and $N_2$ at a short time following the isotopic switch. Obviously, for experimental reasons, it is not possible to get readings directly after the switch (due to perturbations in the gas stream) and thus readings are taken approximately 3 s after the beginning of the switch. At this time the Ar has reached a normalised value of 1, the mixed-labelled products ($^{14}N^{15}N$ and $^{14}N^{15}NO$) have passed through maxima, and the product redistribution is in process. It should be emphasised here that it follows from the mathematical modelling (30) that taking the readings as these mixed species are at their maxima can most accurately compensate for the "experimental nature" of the switch (and its effects on the accuracy of the IDIMP analysis).

Figure 1 shows these plots for $N_2$ and $N_2O$. The results are presented as bar charts showing the normalised production on the ordinate and the number of labelled atoms on the abscissa. In the case of $N_2O$ production it is seen that the initial distribution of the isotopic labels within the $N_2O$ molecules is {0.1, 0.1, 0.8}; i.e., almost all of the $N_2O$ being formed is of the doubly labelled variety. From Eq. [10] this indicates a high occurrence of the mode 0 type of production. This result is in contrast with the deviation from equilibrium result (presented later) in which it is seen that mode 2c is prevalent, and it would be expected that a high level of unlabelled $N_2O$ would be produced from the initial redistribution. However, it must be remembered that the

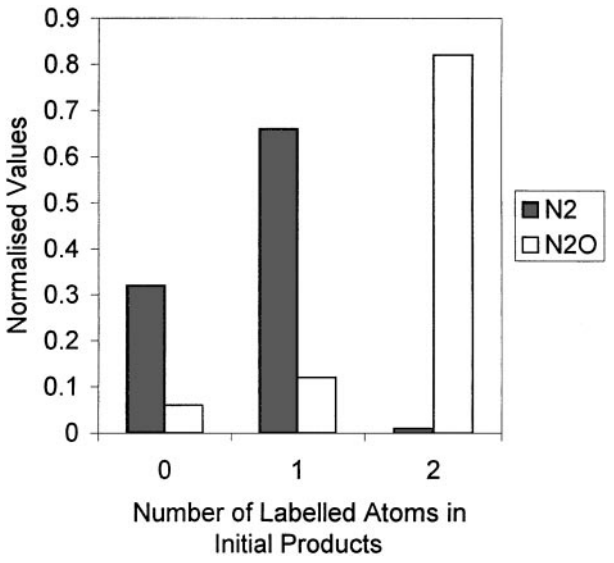


**FIG. 1.** Initial distribution of isotopic molecules of product (IDIMP) following the $^{14}NO + H_2 \rightarrow {}^{15}NO + H_2$ switch over 5% Pt/$SiO_2$ at 60°C. The relative productions of each isotopic species ($^{14}N^{14}N$, $^{14}N^{15}N$ and $^{15}N^{15}N$, ■, as well as $^{14}N_2O$, $^{14}N^{15}NO$ ($^{15}N^{14}NO$) and $^{15}N_2O$, □) are represented.

production of $N_2O$ is relatively rapid and that the choice of time for the "initial" distribution might be too far from the true initial distribution to be of any real value.

In the case of the initial distribution within the $N_2$ molecules it can be seen that the production of the doubly labelled $^{15}N_2$ molecule is hardly seen at all while the production of the mixed labelled molecule is about twice as prevalent as that of the unlabelled one $\{0.32 \pm 0.05, 0.66 \pm 0.05, 0.01 \pm 0.05\}$. In terms of the equations presented above, this can be written as

$$x_0^0 = \chi_{2a} + \chi_{2b} + \chi_{2c} = 0.3 \quad [12]$$

$$x_1^0 = \chi_1 = 0.7 \quad [13]$$

$$x_2^0 = \chi_0 = 0. \quad [14]$$

This indicates that type 1 production operates here (as this produces the initial amount of mixed $N_2$) as does some type 2 (a, b, or c), as this leads to the unlabelled product.

Type 1 production can occur through an impact mechanism in which gaseous NO interacts with a species containing one N atom on the surface. Another possibility for this type is that the reaction might involve the interaction of a weakly adsorbed, pre-adsorbed or physisorbed NO molecule with a species containing one N atom. This would be equivalent to a situation where the reacting NO is in the gaseous state, as the fraction of the labelled pre-adsorbed state would equal that of the gas phase given a fast equilibrium between the two. One possible way to envisage this is through the interaction of an NO "pre-adsorbed" state with some reduced N species on the surface ($NH_x$) where $x = 0$ or 1. Theoretical considerations of where it is possible

to distinguish between these situations are discussed elsewhere (30).

*Integral characteristics of surface participation in the production of $PA_2$.* We can now introduce two integral characteristics which reflect the degrees of surface intermediate (or lattice) participation in the formation of doubly labelled product molecules ($PA_2$) from labelled molecules ($RA_n$) and their connection with the above-introduced initial distribution of isotopic molecules of product.

First is the coefficient of surface production ($C_{PR}$)—this is the average number of surface A atoms which participate in one act of production (desorption) of a molecule $PA_2$. Second is the coefficient of percolation ($C_{PE}$), which is the average number of A atoms of the reactant RA which participate in one elementary act of formation of the product molecule $PA_2$.

In the production of the molecule $PA_2$ there is the obvious connection

$$C_{PR} + C_{PE} = 2. \quad [15]$$

With regard to the five types of production, the percolation and surface production coefficients for each type of production are presented in Table 1. These are derived using IDIMP and the simple equations

$$C_{PR} = 2x_0^0 + x_1^0 \quad [16]$$

$$C_{PE} = x_1^0 + 2x_2^0. \quad [17]$$

Here, the values $x_0^0, x_1^0$, and $x_2^0$ represent the initial normalised fractions of the fully unlabelled, mixed labelled, and fully labelled initial product species, respectively.

In our case (the $NO + H_2$ reaction over 5% $Pt/SiO_2$ at 60°C under steady state conditions) for $N_2$, $C_{PR} = 1.3 \pm 0.1$ and $C_{PE} = 0.7 \pm 0.1$. This simply means that every molecule of $N_2$ produced takes an average of 1.3 N atoms from the surface and an average of 0.7 atoms from the gas phase. It is not feasible to carry out this analysis for the $N_2O$ production because, as has been mentioned, the switch is over too fast for any accuracy to be ensured.

### b. *Temporal Redistribution of Isotopically Labelled Molecules of Product (TRIMP)*

An important characteristic of isotopically labelled molecules with more than one labelled atom of the same element is the extent of the redistribution of the isotopic equilibrium present. This is the situation in our case regarding the product molecules ($N_2$ and $N_2O$). If these molecules are in a state of isotopic equilibrium when the fraction of heavy isotopes ($^{15}N$) in the gas phase is $\alpha$, the equilibrium fraction ($x_i^{eq}$) of the isotopic molecules, e.g., $^{15}N_i{}^{15}N_{(2-i)}$, can be calculated using the binomial distribution (24, 27)

$$x_i^{eq} = \binom{2}{i} \alpha^i (1-\alpha)^{2-i}, \quad [18]$$

where,

$$\binom{2}{i} = \frac{2!}{(2-i)!\,i!} \quad \text{for } i = 0, 1, 2. \quad [19]$$

The most useful probe function for the extent of isotopic equilibrium in an flow system is the deviation ($y_i$) of the fraction of isotopic molecules $^{14}N_{(2-i)}{}^{15}N_i$ ($x_i$) from their equilibrium fraction $x_i^{eq}$. This function was first used by Muzykantov *et al.* (24) for the analysis of isotopic exchange of $O_2$ in a closed system.

$$y_i = x_i - x_i^{eq} \quad \text{for } i = 0, 1, 2. \quad [20]$$

For example, for the $^{14}N^{15}N$ molecule, which contains one heavy atom,

$$y_1 = x_1 - 2\alpha(1-\alpha). \quad [21]$$

When the isotopic molecules $PA_{2-i}{}^*A_i$ are statistically mixed, then $y_i = 0$ for $i = 0, 1, 2$. TRIMP therefore shows the $y_i$ variable for the isotopic molecules of product as a function of time following an isotopic step change, e.g., in our case the $^{14}NO/H_2 \rightarrow {}^{15}NO/H_2$ switch. For a complete description of the composition of isotopic molecules, e.g., $PA_{2-i}{}^*A_i$, we only need to examine one isotopic species, i.e., $PA_2$, $PA^*A$, or $P^*A_2$, in conjunction with the $\alpha$ profile. This is so because the three deviations from equilibrium ($y_0$, $y_1$, and $y_2$) are related (at any time ($t$)) by the relationships

$$y_0(t) + y_1(t) + y_2(t) \equiv 0, \quad y_0(t) \equiv y_2(t), \quad \text{and}$$
$$y_1(t) \equiv -2^* y_0(t) (\text{or } -2^* y_2(t)). \quad [22]$$

This indicates that the largest deviation will be seen for the $y_1(t)$ profile (representing the deviation from equilibrium for the $^{14}N^{15}N$ species) and that the $y_2(t)$ and $y_0(t)$ profiles (which represent the deviations for the $^{14}N^{14}N$ and the $^{15}N^{15}N$ species) will be mirror images of this profile but will be one half as intense. In this work we show both the $y_1(t)$ and the $y_2(t)$ profiles along with the $\alpha$ profile.

Table 1 shows how any variation in the "type of production" is manifested in a change in the TRIMP profiles for a plug flow reactor (30). For types 0 and 2a the isotopic molecules of product are always statistically mixed ($y_1 = y_2 = 0$); for types 1 and 2b there is superproduction of the mixed-labelled species for a time following the switch ($y_1 > 0 > y_2$). Conversely, for type 2c there is subproduction of the mixed-labelled species for a time following the switch ($y_1 < 0 < y_2$). These only apply in the case of "pure" types of production, and any concurrent operation of more than one type of production leads to situations that are more complex. The operation of more than one "type" (for multiroute mechanisms) does *not* generally yield a simple profile resulting from the average of the profiles of the types involved. The imposition of an experimental step change rather than an ideal one here also causes some deviation from "true" $y_i$ profiles. This deviation is only seen at the beginning of the switch when the inverted Ar profile has

not reached a steady value (0 in our case as $^{14}NO$/Ar is removed from the stream).

In the present case, Fig. 2 (a and b), neither the $N_2$ nor the $N_2O$ products are in statistical isotopic equilibrium throughout the course of the whole switch.

In the case of the $N_2$ profiles (Fig. 2a) the deviations appear to be superpositions of more than one mode. There is superproduction of the mixed labelled species directly following the switch (with a maximum value of $y_1$ approximately 20%). This becomes a subproduction roughly 55 s after the switch (with a minimum value of $y_1$ of approximately −3% 175 s after the switch), before statistical redistribution is reached ∼360 s after the switch (at an $\alpha$ value of ∼0.9). We can therefore say that there is not a "pure" type of production operating here. It should also be noted that this generated profile is reproducible, having been repeated several times following the $^{14}NO + H_2 \rightarrow {}^{15}NO + H_2$ switch for these and other experimental conditions.

The mechanism proposed for $N_2$ formation in the $NO/C_3H_6/O_2$ reaction (33) envisages the combination of two N atoms on the surface. This is analogous to mechanism 2a above, in which two equivalent surface species interact to yield the product molecule $N_2$. Theoretical consideration (30) predicts that this situation would lead to no deviation from statistical isotopic equilibrium following the $^{14}NO + () \rightarrow {}^{15}NO + ()$ switch. Thus, we can discount this mechanism as the *sole* source of $N_2$ for the NO + $H_2$ reaction on Pt/$SiO_2$.

As mentioned, it appears that the observed profiles, in which there seem to be two controlling factors governing the sign of the $y_1$ profile, correspond to superpositions of at least two types of production of $N_2$ from NO. We know from the IDIMP analysis that this is the case: $\chi_1 = 0.7$, $\chi_{2a} + \chi_{2b} + \chi_{2c} = 0.3$.

Extensive modelling (30) has shown that there are only *two* "natural" cases where this change of sign (from positive to negative) in the $y_1$ profile can take place. In both cases we must assume that there are two routes with two types of production of $PA_2$ and that the production of $N_2$ follows an "isotopically first/isotopically second"-type series of processes as seen before with respect to the production of $N_2$ and $N_2O$ (Scheme 1).

There is also a connection between the contribution of a route $r$ and the type of production $\chi$. If, for a multiple-route mechanism, a route ($i$) gives *only* a type of production $k$,

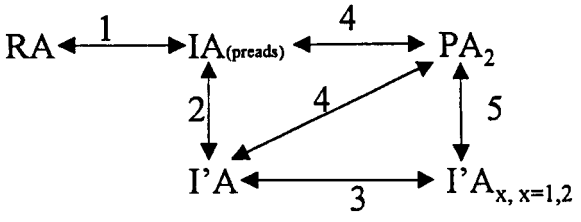


**SCHEME 1**

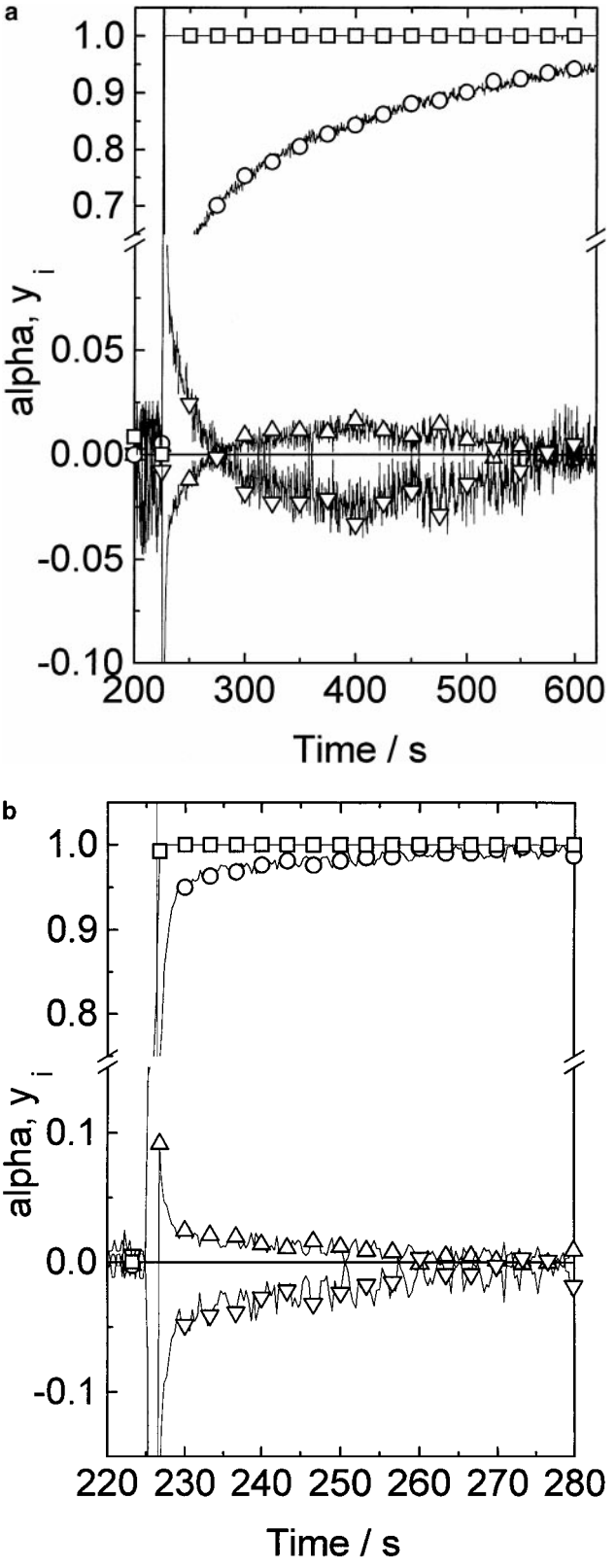


**FIG. 2.** TRIMP plots (in the $y_1$-time coordinate) for (a) $^{15}N_2$ ($y_2$)(△) and $^{14}N^{15}N$ ($y_1$)(▽) and for (b) $^{15}N_2O$ ($y_2$)(△) and $^{14}N^{15}NO$ (and $^{15}N^{14}NO$) ($y_1$) (▽) following the same experiment shown in Fig. 1. Profiles for the respective $\alpha$ function (○) and the inverted Ar trace (□) are also shown.

then the contribution of this route $r_i = \rho_i / \Sigma\rho_i = \chi_k$, where $i = 1, 2, \ldots N$ (number of routes) and $k = 0$, 1, 2a, 2b, 2c (number of types of production).

Processes that can lead to a superproduction of $^{14}N^{15}N$ (as seen in the isotopically first $N_2$ produced) can be type 1 or type 2b production. However, we know that we have a contribution of type 1 production from the IDIMP results. The *only* "pure" type of production that leads to a subproduction of $^{14}N^{15}N$ is that which comes from a coupled intermediate on the surface (type 2c). Thus it is possible that the formation of $N_2$ takes place through two routes, one being type 1 and one being type 2c, with the former leading to isotopically first $N_2$ and the latter leading to isotopically second. Our modelling shows (30) that the interaction of these two types of production leads to a $y_1$ profile that changes sign in a qualitatively similar manner to that seen here (see Fig. 3).

Also from modelling it follows that the interaction of routes with a type 1 production (in which $RA + IA \rightarrow PA_2$) and a type 2a production (in which $2IA \rightarrow PA_2$) can also produce a profile qualitatively similar to that seen in Fig. 2a

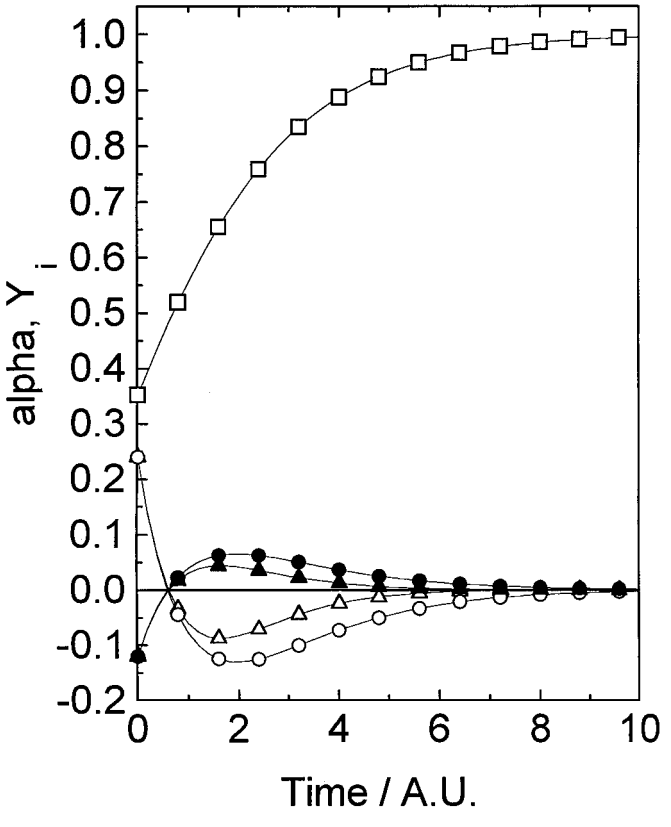


**FIG. 3.** Modelled $\alpha(PA_2)$, $y_1$, and $y_2$ profiles from the superposition of types of production $1+2a$ and $1+2c$ (Scheme 1): $\alpha$ profile (□), $y_1$ profile ($1+2a$ (△) $1+2c$ (○)), $y_2$ profile ($1+2a$ (▲) $1+2c$ (●)). Results are modelled setting the contribution of type 1 process at 0.7. All steps are irreversible, the rate of adsorption is set at 1, $C(IA)_{preads}$ is small, $CI'A = 1$, $CI''A_x = 0.25$ (with respect to the number of A atoms), and all units are unidimensional.

(see Fig. 3). This is interesting since "pure" type 1 leads to an overproduction of $^{14}N^{15}N$ and "pure" type 2a leads to a statistical mixing of isotopic molecules of product. However, when both types are operating together, the $y_1$ profile changes sign and there is a subproduction of $^{14}N^{15}N$ seen for a time after the switch. Scheme 1 shows these two combinations of types of production.

Briefly, this refers to a situation where RA adsorbs on the catalyst surface to form a physisorbed species (IA) (step 1). This then fully adsorbs on the surface (step 2 to form I′A). Now it can interact with a gaseous RA molecule (or the physisorbed IA species) to form $PA_2$ (step 4—producing the "isotopically first" component of $PA_2$ with a type 1 production, as discussed earlier). It can also go on (step 3) to form a second type of intermediate $I'A_x$ ($x = 1$ or 2). If $x = 1$, then this species can then interact with another $I'A_x$ species to form $PA_2$ (isotopically second in a type 2a production—step 5). If $x = 2$, then this species can itself form $PA_2$ (isotopically second in a type 2c production—step 5).

Thus, we will need to discriminate between these two situations (superpositions of types $1+2a$ and types $1+2c$) in order to get a picture of the actual mechanism of $N_2$ formation under reaction conditions. Figure 3 shows modelling results for the $y_1$, $y_2$, and $\alpha$ profiles expected from a combination of $1+2a$ ($y_1$, △; $y_2$ ▲) and $1+2c$ ($y_1$, ○; $y_2$ ●). These are modelled on the assumption that the contribution of type 1 is $\chi_1 = 0.7$ (from the IDIMP analysis), and in both cases the $\alpha$ profile (□) is the same. Figure 4 shows these modelled data presented as $y_1$ ($y_2$) as a function of $\alpha$.

One difference between these profiles (Fig. 3) is that the minimum value of the $y_1$ profile is lower in the second case (superposition of 1 and 2c) than in the first (superposition of 1 and 2a). Another difference is that in the former case ($1+2a$) statistical equilibrium ($y_1 = y_2 = 0$) is reached when the $\alpha$ value is ~0.95, while in the latter case ($1+2c$) the molecules of product are not statistically mixed until the $\alpha$ value approaches 1. This is best seen in Fig. 4. Another way of pointing this out is to observe that in the $1+2c$ case the $y_1$ ($y_2$) profile, upon changing sign, is approximately symmetrical between this value of $\alpha$ and $\alpha = 1$. The $y_1$ ($y_2$) profile is not symmetrical (between the value of $\alpha$ at which it changes sign and reaches a value of $\alpha = 1$) in the case where $1+2a$ operates as it reaches a value of zero before $\alpha = 1$.

Note here that the approximately symmetrical form for $y_i$ in the $y_i - \alpha$ graphical presentation is a common feature for the superposition of $1+2c$. This difference in symmetry (between $1+2c$ and $1+2a$) will be more pronounced when the concentration of the $I'A_x$ is relatively low. In both cases the absolute value of the minimum for $y_1$ (or the maximum for $y_2$) will be lower when the $I'A_x$ concentration is low.

The $y_i$ versus $\alpha$ profiles derived from the present data are shown in Fig. 5. The $y_1$ ($y_2$) profiles are not symmetrical following the change in sign. Indeed isotopically statistically mixed $N_2$ molecules of product are formed when $\alpha(N_2) \sim 0.95$. Thus our experimental data supports

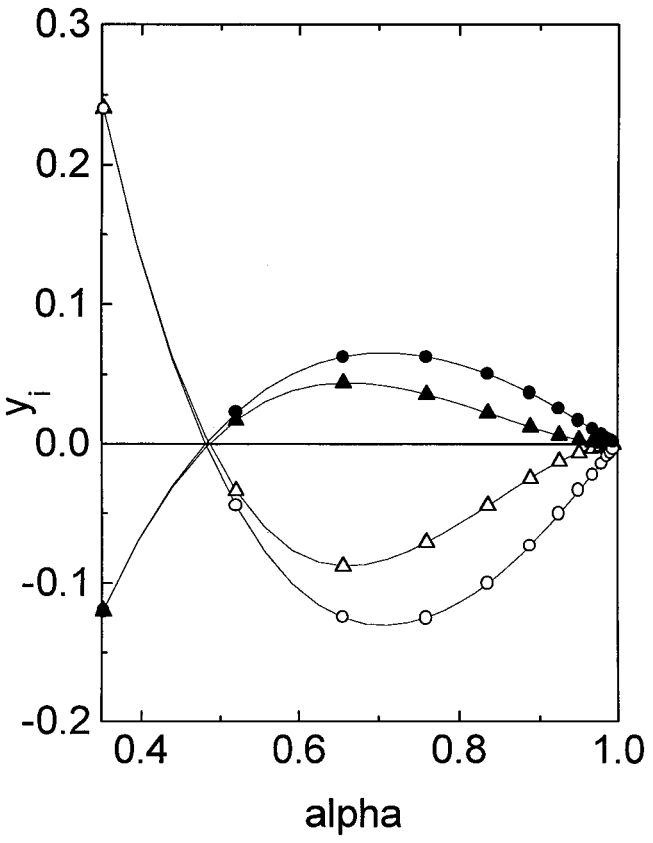


**FIG. 4.** The data in Fig. 3 plotted as a function of $y_i$ against $\alpha$: $y_1$ profile (1 + 2a (△) 1 + 2c (○)), $y_2$ profile (1 + 2a (▲) 1 + 2c (●)).

a two-routes mechanism for the formation of $N_2$. One of these routes gives a type 1 production while the second gives a type 2a production.

The temporal redistribution profile for the mixed-labelled $N_2O$ species (Fig. 2a) is lower than would be expected from the above-mentioned statistical equilibrium calculation. Conversely, the unlabelled and doubly labelled $N_2O$ species obviously show the reverse behaviour, with production profiles consistently higher than would be expected from a statistical equilibrium mixture. Once the switch is over (regarding the product molecule of interest) then statistical equilibrium is restored; i.e., all the molecules formed are doubly labelled and the $\alpha$ value for the product molecule is equal to 1.

This is not what would be expected from the proposed mechanism of $N_2O$ formation over supported Pt catalysts from the NO/$C_3H_6$/$O_2$ reaction (33). Therefore, we can say that a different mechanism of $N_2O$ formation operates in the NO + $H_2$ reaction over these catalysts. This is indicative of a type 2c production.

### *c. Semilogarithmic Plots of $\bar{\alpha}$ versus Time*

These plots involve plotting the function $|\ln|(\bar{\alpha})||$ against time following the isotopic switch (where $\bar{\alpha}$ represents the $(1-\alpha)$ profile in the case of a $^{14}NO \rightarrow {}^{15}NO$ switch and the $\alpha$ profile in the case of the reverse $^{15}NO \rightarrow {}^{14}NO$ switch). In this case $\bar{\alpha}$ refers to $1-\alpha$ as the switch considered is $NO + () \rightarrow {}^*NO + ()$. This gives information about the reaction network leading to products. This presentation is derived from classical isotopic exchange analysis and is used to reflect the heterogeneity of the surface (or lattice) intermediates (30).

Specifically, at steady state, it gives information regarding the presence of a buffer step (in which a pool of inactive intermediates could be formed, in a reversible process, from a pool of active intermediates) or the presence of a consecutive mechanism (in which one pool of intermediates goes on to form another pool of intermediates before forming a product molecule), or, for example, the presence of a mechanism in which there is only one intermediate.

In each case the semilogarithmic plot of $\bar{\alpha}$ versus time has a different shape. In the first case the curve is convex, in the second it is concave, and in the third a straight line is obtained. A mechanism in which there are parallel routes leading to product and both show reversibility also yields a convex plot. Details of these different possibilities can be found in Table 2. The following shapes are expected. In the case of irreversible adsorption of reactant and desorption of product, for a one-pool mechanism $\alpha(t)$ is a function of one exponent (19) (therefore the semilogarithmic plot of $\bar{\alpha}$ versus

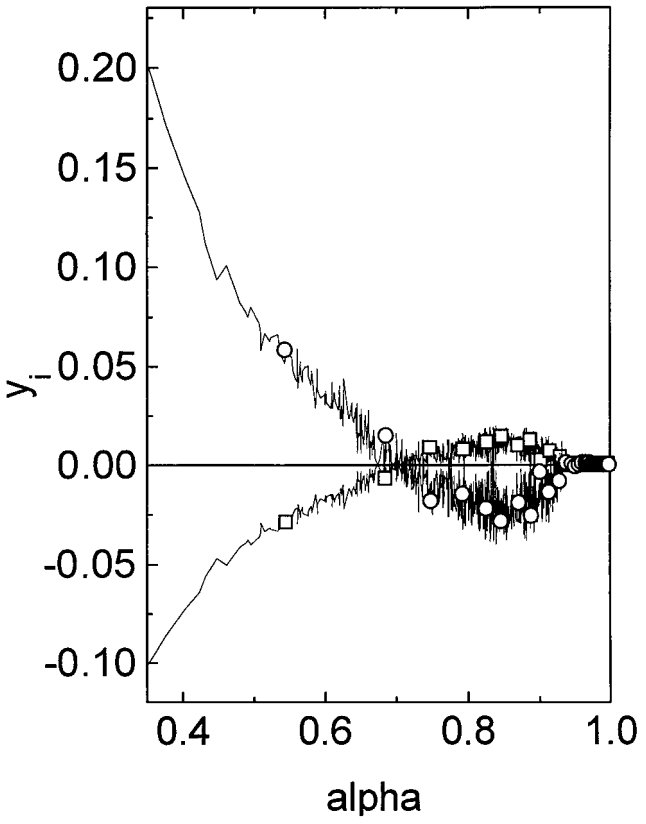


**FIG. 5.** Experimental data plotted as shown in Fig. 4, i.e., $y_i$ as a function of $\alpha$, $y_1$ (○), $y_2$ (□).

time is linear). Buffer (19) and parallel (20) pools result in $\alpha(t)$ being the sum of two exponents (semilogarithmic plot of $\bar{\alpha}$ versus time is convex), and in the case of consecutive pools then $\alpha(t)$ is the difference of two exponents (19) (semilogarithmic plot of $\bar{\alpha}$ versus time is concave). Combinations of these mechanisms lead to semilogarithmic plots of $\bar{\alpha}$ versus time that are superpositions of the former plots.

Our results are generated from modelling reversible cases of adsorption of RA and desorption of $PA_2$ (when $\alpha(t)$ *cannot* be represented in exponential form), and these show qualitatively similar shaped features to the situations discussed above (34). In the case of reversible adsorption of reactant, a situation that has heretofore been ignored, then the same transformation of the profile of the unreacted reactant (RA) can also yield information regarding the reaction network (34). As was the case in the IDIMP and TRIMP studies, the nature of the "gas-phase holdup" effects the shape of these profiles. However, in this case the effect is far less severe. The relationship between the "gas-phase holdup" and the $\alpha$(product) response (in the case of irreversible adsorption/desorption) has been previously derived (35).

In our case the semilogarithmic plot of $\bar{\alpha}$ versus time for the production of both $N_2$ and $N_2O$ is shown with a standard Ar response in Fig. 6. Both of these are convex, and thus both sets of intermediates (of $N_2$ and $N_2O$) must have buffer states or possibly are formed from parallel mechanisms such as those detailed in the fourth row of Table 2. It is seen that the $N_2O$ profile is far sharper than that of the $N_2$. This is as expected as the transient in $N_2O$ is itself far quicker than that for $N_2$ ($N_2O$ is the isotopically first product). A value of 4 in the semilogarithmic plot of $\bar{\alpha}$ versus time is indicative of 99% transference of the heavy ($^{15}N$) isotope into the product molecules. Thus in the reaction network scheme we must, with a high probability, allow for the presence of an intermediate buffer state for $N_2O$ and for $N_2$ production, and both buffers cannot be represented by the same species.

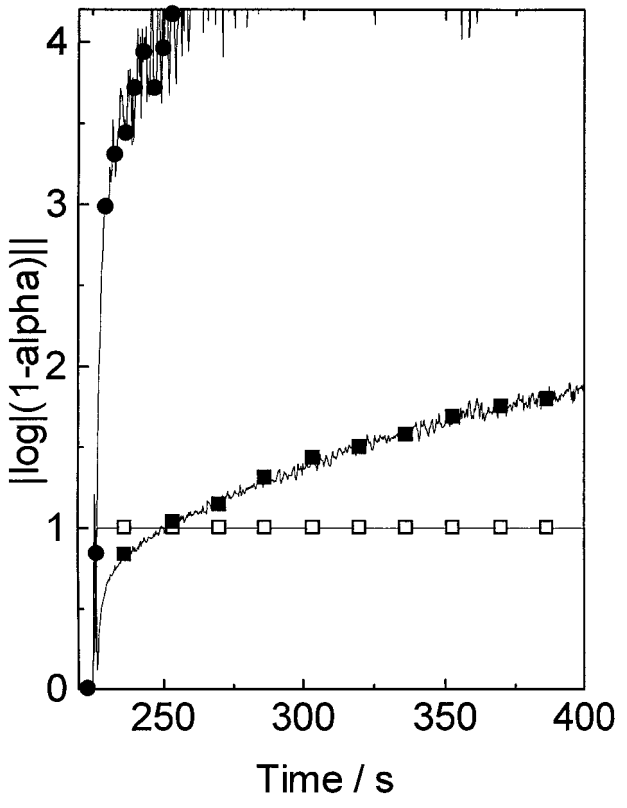


**FIG. 6.** Semilogarithmic plots of the function $|\ln|(\bar{\alpha})||$ against time for the product molecules $N_2O$ and $N_2$ as well as an Ar profile following the $^{14}NO + H_2 \rightarrow {}^{15}NO + H_2$ switch over 5% $Pt/SiO_2$ at 60°C: $N_2$ (■), $N_2O$ (●), inverted Ar (□).

The formation of the buffer can be considered as NO adsorbed on different interconvertible sites, one of which is active for further reaction/desorption and one of which is not. This could be a physically different site on the catalyst (e.g., at a different metal site or at the metal–support interface, but not the support itself as $SiO_2$ does not adsorb significant quantities of NO) or a site that is periodically modified under reaction conditions, e.g., $NO_{ads} \longleftrightarrow NO_{2ads}$. At steady state the concentration of the buffer must be a constant; i.e., its rate of formation must equal its rate of removal.

**TABLE 2**

**The Variations Expected in the Semilogarithmic Plots of the Function $|\ln|(\bar{\alpha})||$ against Time for Various Mechanisms for the Transformation of Reactant R into Product P**

| Label | Mechanism | Shape of semilogarithmic plot (with time) $\lvert\ln(\bar{\alpha}(t))\rvert$ |
|---|---|---|
| Direct | $R \Leftrightarrow I_1 \Leftrightarrow P$ | Straight line |
| Consecutive | $R \Leftrightarrow I_1 \Leftrightarrow I_2 \Leftrightarrow P$ | Concave curve |
| Buffer | $R \Leftrightarrow I_1 \Leftrightarrow P$ <br> $\Updownarrow$ <br> $I_2$ | Convex curve |
| Parallel | 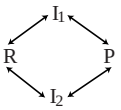 | Convex curve |



*Note.* See text for details.

## PROPOSED MECHANISM

From the above analyses and those presented in the previous paper (13) we can outline a reaction scheme for the production of $N_2$, $N_2O$, and $NH_3$ during the $NO + H_2$ reaction.

With respect to the formation of $N_2O$, from *the present* analysis, we can say:

- There is a buffer state present in the reaction network (as qualitatively determined from the semilogarithmic plots of $\bar{\alpha}$ versus time).

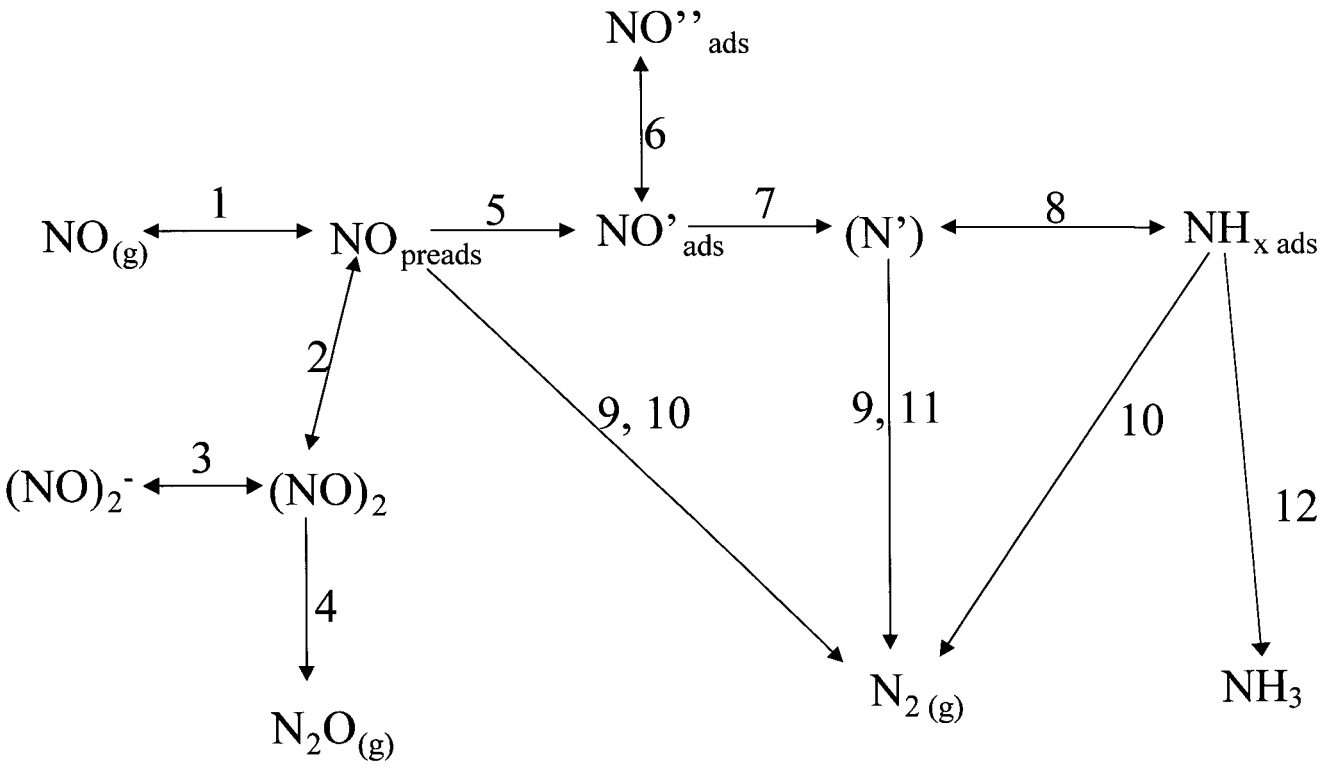


**SCHEME 2.** Network of NO conversion into $N_2O$, $N_2$, and $NH_3$ over 5% Pt/$SiO_2$ in the NO + $H_2$ reaction as derived from SSITK analysis.

- The formation is very rapid on the surface (relative to $N_2$ production).
- A final intermediate on the surface in the production of $N_2O$ contains two nitrogen atoms (from the TRIMP data).

With respect to the formation of $N_2$, from *the present* analysis we can say:

- There is buffer state on the catalyst for $N_2$ precursors (from semilogarithmic plots of $\bar{\alpha}$ versus time). Also we can say that this buffer is not the same one as that seen for the production of $N_2O$, as this is a far slower process on the surface.
- There are at least two types of production of $N_2$ on the catalyst. One of these is through a type 2a process, i.e., a route where two equivalent species on the surface interact to form $N_2$, and one is through type of production 1—an "Impact" route, i.e., where gaseous or physisorbed NO interacts with an NO-derived species on the surface to form $N_2$ (from the temporal redistribution plots and the initial distribution data). The contribution of type 1 is around 70% while that of type 2a is near 30%—as determined from the IDIMP analysis;
- The concentration of final intermediates which form $N_2$ with type of production 2a is relatively small. We can say this as there is only a small negative deviation from equilibrium of the $y_1$ values from the TRIMP analysis;
- The $N_2$ formation through the "impact" type of production (type 1) produces $N_2$ "isotopically first" while the "equivalent intermediates" mechanism (type 2a) produces $N_2$ isotopically second.

Scheme 2 is a general outline of the network of the N-containing species, following them from gaseous NO through the various surface intermediates and showing production of $N_2$, $N_2O$, and $NH_3$. The scheme takes into account the above-mentioned points, as well as the conclusions from the previous paper (13).

In this scheme the adsorption of NO goes through a pre-adsorbed state (step 1). The pre-adsorbed (weakly bonded) NO can dimerise to produce dinitrosyl $(NO)_2$-type species (step 2). This can be stabilised—perhaps by the addition of an electron from the Pt particles (yielding an $(NO)_2^-$ species). This can be considered as a buffer step (step 3). The $(NO)_2$ species could also dissociate to the $N_2O_{(g)}$ and leave behind an $O_{ads}$ species (step 4). The overall concentration of surface intermediates $(NO)_2$ and $(NO)_2^-$ must be quite low.

The pre-adsorbed state can also move to a more "fully" adsorbed state on the metal surface (step 5). From here it can either enter a buffer state (step 6) from which it can re-emerge later, or it can become more reduced (by the formation of N, step 7).

This species (formed in step 7) could, in the presence of excess $H_2$, become further hydrogenated (step 8, forming $NH_x$). Further hydrogenation would result in the generation of $NH_3$ (step 12). However, it is considered here that its primary reaction route is to interact with the pre-adsorbed

(or gaseous) NO to form $N_2$ (in the modified "impact" route, step 10). Another possible method of forming $N_2$ via the "impact route," as detailed in step 9, could be the interaction of the physisorbed NO with the N′ species formed via NO decomposition. Both of these routes give the type 1 production of $N_2$.

We also need to account for the production of $N_2$ from two intermediates that are equivalent and stable on the surface (type of production 2a). This could be formed by an interaction (step 11) between two of the N′ species formed in step 7.

We can also comment on the rates and reversibility of certain of the steps from the SSITKA and NSSITKA in the previous paper (13). For example, we can say that the rate of the $N_2O$ formation is of the same order as the net rate of NO adsorption. This, coupled to the information that the overall concentration of $N_2O$ intermediates is small (13), would explain how the $\alpha$ $N_2O$ profile and the $^{15}NO$ profile are the same following the $^{14}NO \rightarrow {}^{15}NO$ switch.

We can also say that step 2 and step 3 are reversible but that step 5 is irreversible. This we have seen from the stopped flow switching experiments (13), in which the $N_2O$ precursors could be transformed into $N_2$ precursors by the removal of the gaseous NO. The representation of the coupled intermediate $(NO)_2$ and its stabilisation by donation of an electron have been postulated previously (36) and are chemically feasible.

## CONCLUSIONS

A mechanism has been proposed for the $NO/H_2$ reaction over $Pt/SiO_2$ catalysts that explains all the observed features from the SSITKA and temperature programmed analysis. This involves two routes (with types of production 1 and 2a) for the formation of $N_2$. The first of these is via an "impact" mechanism where gaseous (or weakly adsorbed) NO interacts with a surface species, and the second involves interaction of two equivalent species on the surface. The contribution of the Eley–Rideal-like "impact" route is roughly 70% while that of the Langmuir–Hinshlewood route is roughly 30%. $N_2O$ is formed from the decomposition of a surface species containing 2 N atoms (with a 2c type of production). The formation of $N_2O$ is far faster on the surface than that of $N_2$ and its surface intermediates are far less stable than those of $N_2$.

At 60°C, under steady state conditions every molecule of $N_2$ formed during the $NO + H_2$ reaction takes an average of 1.3 atoms from the surface intermediates and an average of 0.7 atoms from gas-phase NO ($C_{PR} = 1.3$, $C_{PE} = 0.7$).

## ACKNOWLEDGMENTS

We are grateful to the EPSRC for supporting this research through contract GR/K70403. A.A.S. thanks NATO and The Royal Society for providing a fellowship (NATO/96A).

## REFERENCES

1. Hanssen, K. F., Blekkan, E. A., Schanke, D., and Holmen, A., *Stud. Surf. Sci. Catal.* **109**, 193 (1997).
2. Bajusz, I. G., Kwik, D. J., and Goodwin, J. G., *Catal. Lett.* **48**(3-4), 151 (1997).
3. Efstathiou, A. M., and Verykios, X. E., *Appl. Catal. A General* **151**(1), 109 (1997).
4. Nibbelke, R. H., Scheerova, J., de Croon, M. H. J. M., and Marin, G. B., *J. Catal.* **156**, 106 (1995).
5. Ali, S. H., and Goodwin, J. G., *J. Catal.* **170**(2), 265 (1997).
6. Oukaci, R., Blackmond, D. G., Goodwin, J. G., Jr., and Gallagher, G. R., *in* "Catalytic Control of Air Pollution," Ch. 5, pp. 61–72. Am. Chem. Soc., Washington, DC, 1992.
7. Frost, J. C., Lafyatis, D. S., Rajaram, R. R., and Walker, A. P., *in* "4th International Congress on Catalysis and Automotive Pollution Control, Brussels, April 1997," Vol. 1, p. 129, O14, 1997.
8. Efstathiou, A. M., and Fliatoura, K., *Appl. Catal. B Environ.* **6**(1), 35 (1995).
9. Janssen, F. J. J. G., Van Den Kerkhof, F. M. G., Bosch, H., and Ross, J. R. H., *J. Phys. Chem.* **91**(27), 6633 (1987).
10. Kumthekar, M. W., and Ozkan, U. S., *J. Catal.* **171**(1), 54 (1997).
11. Burch, R., and Sullivan, J. A., *J. Catal.* **182**(2), 489 (1999).
12. Burch, R., Shestov, A. A., and Sullivan, J. A., *J. Catal.* **182**(2), 497 (1999).
13. Burch, R., Shestov, A. A., and Sullivan, J. A., *J. Catal.* **186**, 354 (1999).
14. Happel, J., *Chem. Eng. Sci.* **33**, 1567 (1978).
15. Bennett, C. O., *in* "Catalysis Under Transient Conditions" (A. T. Bell and L. L. Hegedus, Eds.), ACS Symposium Series, Vol. 178, p. 1. Am. Chem. Soc. Washington, DC, 1982.
16. Biloen, P., *J. Mol. Catal.* **21**, 17 (1983).
17. Godfrey, K., "Compartmental Models and their Application." Academic Press, London, 1983.
18. Happel, J., Walter, E., and Lecourtier, Y., *I&EC Fundam.* **25**, 704 (1986).
19. Happel, J., Walter, E., and Lecourtier, Y., *J. Catal.* **123**, 12 (1990).
20. Shannon, S. L., and Goodwin, J. G., Jr., *Chem. Rev.* **95**, 677 (1995).
21. Mirodatos, C., *Catal. Today* **9**, 83 (1991).
22. Kemball, C., *Adv. Catal.* **11**, 223 (1959).
23. Klier, K., Novakova, J., and Jiru, P., *J. Catal.* **2**, 479 (1963).
24. Muzykantov, V. S., Popovskii, V. V., and Boreskov, G. K., *Kinet. Catal.* **5**(N4), 624 (1964).
25. Boreskov, G. K., and Muzykantov, V. S., *Ann. N.Y. Acad. Sci.* **213**, 137 (1973).
26. Muzykantov, V. S., *React. Kin. Catal. Lett.* **33**, 937 (1987).
27. Boreskov, G. K., *in* "Catalysis, Science and Technology," Vol. 3, p. 39. Springer-Verlag, New York, 1982.
28. Winter, E. R. S., *J. Chem. Soc. A*, 2889 (1968).
29. Ozaki, A., *in* "Isotopic Studies of Heterogeneous Catalysts." Academic Press, New York, 1977.
30. Shestov, A. A., Burch, R., and Sullivan, J. A., to be submitted.
31. Mirodatos, C., *J. Phys. Chem.* **90**, 681 (1986).
32. Mirodatos, C., Dalmon, J. A., and Martin, G. A., *J. Catal.* **105**, 405 (1987).
33. Burch, R., Sullivan, J. A., and Watling, T. C., *Catal. Today* **41**(1-2), 13 (1998).
34. Shestov, A. A., Burch, R., and Sullivan, J. A., "Reaction Kinetics and the Development of Catalytic Processes," Belgium, April 19–21, 1999.
35. Shannon, S. L., and Goodwin, J. G., *Appl. Catal. A General* **151**, 3 (1997).
36. Acke, F., Ph.D. thesis, University of Göteborg, Sweden.